

A 3D Bioprinted Tumor Model for Immuno-oncology Applications

Shubhankar Nath, PhD and Itedale Namro Redwan, PhD
CELLINK LLC, Boston, MA, USA

Abstract

T cell-based therapies are rapidly developing into an effective first-line treatment option for many cancers. In recent years, several therapeutic antibodies and small molecules targeted to immune checkpoints, have been approved by the FDA for clinical use to complement and increase T cell targeting and effectiveness. Preclinical screening of these immune checkpoint inhibitors requires robust *in vitro* tumor models to evaluate T cell killing efficiency. However, traditional 2D tumor models often lack the biological relevance and complexity to predict *in vivo* or clinical outcomes. 3D bioprinting platforms, among many other 3D culture methods, offer the potential to automate the screening of various molecules and drugs in more physiologically relevant tissue models. Here, in this proof-of-concept study, we described a syngeneic bioprinted tumor model of murine lung cancer to evaluate an immune checkpoint inhibitor (PD-1) in a 3D T cell cytotoxicity assay. T cell concentration dependent killing was observed within bioprinted tumors, and the addition of immune checkpoint antibodies further enhanced T cell killing efficacy. It is suggested that bioprinted T cell cytotoxicity assays may allow researchers to screen checkpoint inhibitors in more efficient and translational models.

1

Introduction

T lymphocytes (T cells) play a critical role in achieving long-term immunity against infectious diseases as well as cancers. T cells can recognize specific antigens in the context of major histocompatibility complex (MHC) molecules on the surface of infected or cancerous cells. This specific recognition leads to secretion of toxic granules from the T cells to specifically kill the target cells. Traditionally, T cell killing (cytotoxicity) assays have been performed using target cells grown in two-dimensional (2D) monolayers (Golstein, 2018). These 2D assays quickly and easily perform end-point analysis by imaging or other means. However, inside the human body, T cell-mediated killing of target cells occurs in a three-dimensional (3D) environment, which attributes to additional barriers for T cells to migrate or infiltrate into the core of the 3D tissue. Thus, 3D T cell cytotoxicity assays are more physiologically relevant and thought to better predict the outcome of *in vivo* experiments. For clinical testing of immunostimulatory agents, there has been increased interest in performing cytotoxicity assays using 3D tumor models.

Recent developments in checkpoint blockade therapy have revolutionized the field of cancer therapy where immune checkpoints are inhibited to enhance T cell-mediated killing of tumor cells (Topalian, 2016). Several checkpoint inhibitors, such as anti-PD1 and anti-PD-L1 antibodies, have been approved for clinical use (Sharon, 2014). However, there remains an unmet need to develop high-throughput T cell cytotoxicity assays to screen such inhibitors quickly and cost efficiently.

Several 3D tumor models, including spheroids, hanging droplets and microfluidic chip models have been studied for T cell cytotoxicity assays. For example, collagen-fibrin gel was used to grow cancer cells in a 3D environment to determine the absolute concentration of T cells needed to kill all the cancer cells (Budhu,

2010). More recently, microfluidic spheroid culture was used for *ex vivo* profiling of immune checkpoint blockade (Jenkins, 2018). While these models show promise in mimicking certain aspects of the *in vivo* setting, they are often low-throughput or fail to consider the critical role of the extracellular matrix (ECM) in tumor biology.

Bioprinting is an emerging technology that enables researchers to automate fabrication of tumor constructs for the screening of anticancer drugs or immune-stimulatory agents. The technique deposits a cell-laden ECM material, commonly known as a bioink, blended with tumor cells and subsequently cured chemically or thermally to provide mechanical strength to the printed structure. Here, we explore the potential of bioprinting technology for 3D T cell cytotoxicity assays to aid in evaluating immune checkpoint inhibitors.

Materials and Methods

Cell preparation

Mouse lung cancer cell line (LLC-1) and syngeneic OT-1 T cells were selected for this project. Both cell types are in C57BL/6 background. Lewis lung cancer cells (LLC-1) were obtained from the American Type Culture Collection (ATCC) and cultured according to suggested protocols and passaged every 3 to 4 days. To facilitate the imaging of the live tumor cells, a plasmid encoding red fluorescent protein (RFP) was introduced into LLC-1 cells to generate stable LLC-RFP cells. LLC-RFP cells (“LLC-1” thereafter) were used for the rest of the experiments. OT-1 splenocytes were cultured and primed for 5 days using 0.75 µg/mL SIINFEKL (Ova) peptide (New England Peptide) following a previously published protocol (Nath, 2016). Primed cytotoxic T lymphocytes (CTLs) were used without further purification in co-culture studies on Day 5.

Bioink preparation and bioprinting

Collagen I (CELLINK) was neutralized and mixed with 10^6 LLC-1 cell per mL of collagen. All components, including syringes, needles and tips were kept on ice until ready for use. A temperature-controlled printhead (TCPH) was set to 8°C while the printbed was set to 10°C. Three-dimensional LLC-1 tumors were bioprinted using the droplet function on the BIO X (Software version 1.8) in 96-well plates (n=3) (see **Figure 1**). Following the printing, the 96-well plate was transferred to a 37°C humidified incubator for 20 minutes to allow collagen polymerization. Next, 200 µL of DMEM media was added to each well. Media was refreshed every 3 days. The tumors were grown for 5 days before they were used in co-culture with T cells.

2

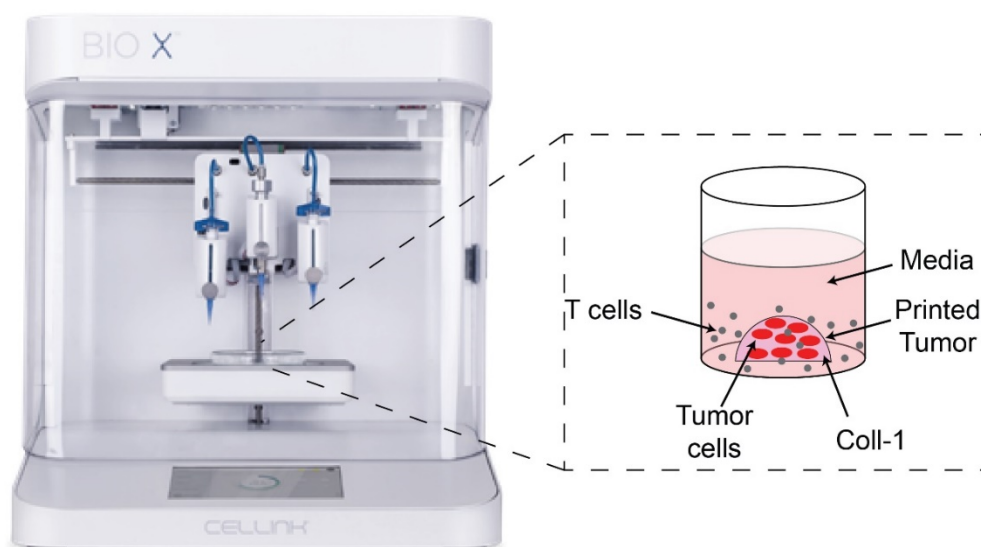


Figure 1. Three-dimensional (3D) bioprinting of tumors. Lewis lung cancer cells (LLC-1) were printed with collagen using the droplet printing function of the BIO X. The collagen droplets (tumors) were cured thermally and maintained in DMEM media for 5 days before using them in co-cultures with T cells.

On Day 4, printed tumors were incubated with 1 µg/mL of SIINFEKL peptide for 24 hours to allow the tumor cells to express the cognate antigen. On Day 5, printed tumors were washed and co-cultured with T cells at different effector to target (E:T) ratios (from 0 to 5) for 48 hours. For positive control, tumors were incubated with etoposide or TNFα to induce cell death by apoptosis. The negative control wells did not receive any T cells or apoptotic inducers. For antigen specificity, tumors in a few (n=8) wells were not treated with SIINFEKL but received the primed T cells.

For immune checkpoint assay, primed T cells were pretreated with 1 µg/mL of anti-PD-1 antibody (clone RMP1-14, InVivoMab) for 1 hour before they were added into the co-culture with tumors (n=8). An IgG isotype control was kept for comparison.

Imaging and statistics

Loss of RFP fluorescence was used as a readout of tumor cell death as described previously (Steff, 2001; Strebel, 2001). Imaging was performed using the EVOS Auto 2 fluorescent microscope. Fluorescence intensity was measured using ImageJ software (NIH) and graphs were translated and prepared using Graphpad Prism 8. The results were statistically measured in Prism by using Student's t-test and the data were expressed as the mean ±SEM.

Results and Discussion

Tumor cell growth and spheroid formation

The droplet function on the BIO X was able to automate the dispensing of consistent collagen-tumor droplets in 96-well plates. Uniformity in droplet shape and well placement aided in the overall microscopy and analysis workflow. Printed tumors were imaged for RFP fluorescence and stained with Calcein AM to determine cell viability. The results shown in **Figure 2** indicate that LLC-1 cells were viable in the printed tumors at Day 5. Moreover, the cells were confined within the collagen rather than escaping the structure to grow on 2D surfaces.

3



Figure 2. Tumor cell growth and viability. Printed tumors were imaged for RFP fluorescence and stained with Calcein AM to determine cell viability at Day 5 before T cell screening.

T cell cytotoxicity assay in 3D

T cell-mediated cytotoxicity was validated both quantitatively and qualitatively. When tumors were co-cultured with T cells, a T cell concentration-dependent decrease in tumor cell viability was observed (see **Figure 3A**). At 5:1 (E:T) ratio, which represents 10⁶ CTLs/well, a statistically significant (p=0.0003) reduction (~30%) in tumor viability was observed compared to the no CTL control. Representative images of printed tumor in the presence or absence of T cells are shown in **Figure 3B** which exhibits qualitative decrease in RFP fluorescence when T cells were present in the co-culture. The T cells were able to attach to the collagen barrier and interact with cancer cells within the 3D ECM environment.

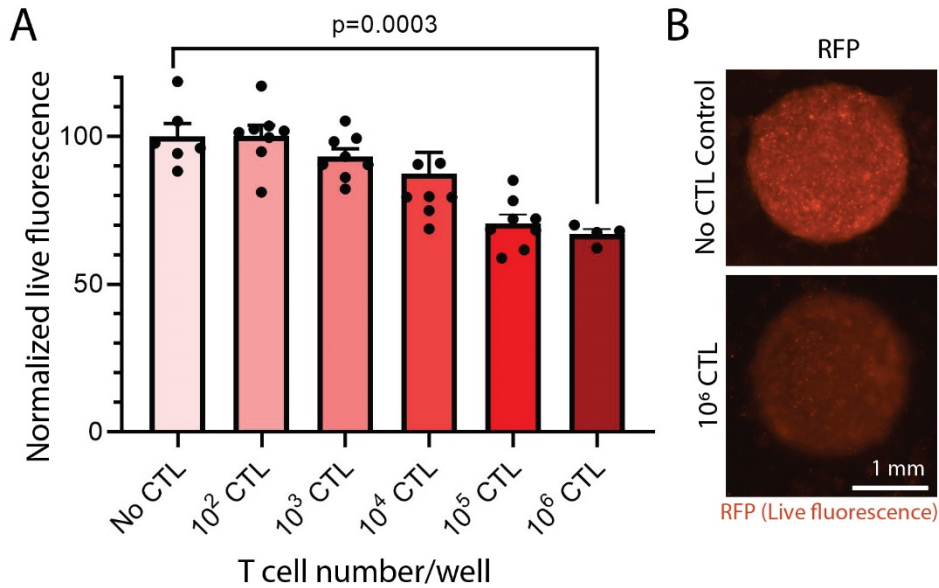


Figure 3. T cell cytotoxicity assay using 3D bioprinted tumor model at Day 5. **(A)** A T cell concentration-dependent decrease in tumor cell viability was observed as determined by loss in RFP fluorescence. The number of CTL represents total CTL per well. **(B)** Representative images of printed tumor in the presence or absence of T cells are shown. Images were taken using the same acquisition parameters.

Immune checkpoint assay

To expand upon the utility or limitation of T cell killing, tumors were co-cultured with primed T cells pretreated with anti-PD1 antibody at an E:T ratio of 5:1. As shown in **Figure 4**, blockade of PD-1/PD-L1 axis using an anti-PD1 antibody exhibited an increase in T cell-mediated killing of tumor cells ($p=0.0039$) compared to the isotype control. Thus, primed T cells were able to attach to the collagen barrier, infiltrate and kill tumor cells more efficiently as a result of PD-1 checkpoint blockade.

4

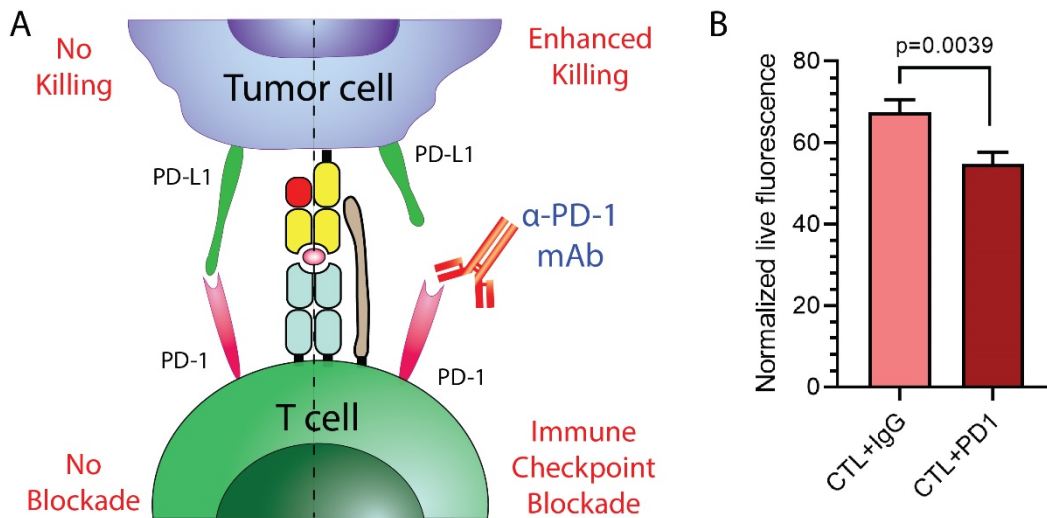


Figure 4. Immune checkpoint blockade. **(A)** A schematic of immune checkpoint blockade assay is shown. Monoclonal anti-PD1 antibody blocks the interaction between PD1 and PD-L1, resulting in enhanced killing of the tumor cells by T cells. **(B)** 3D bioprinted tumor cells were co-cultured with primed T cells at an E:T ratio of 5:1 in the presence of either IgG isotype control or anti-PD1 antibody. PD1 blockade showed enhanced killing of the target cells.

Conclusions

- 3D bioprinting technology can be used in a T cell cytotoxicity assay to print RFP-labeled murine lung cancer cells with collagen.
- Bioprinted tumor cells remained confined and viable within a collagen matrix. A T cell concentration-dependent increase in cytotoxicity was observed.
- The use of an anti-PD-1 antibody enhanced T cell-mediated killing efficiency as described in the literature.
- The T cell cytotoxicity assay is compatible with high-content imaging workflows and can also be adapted for other tumor models, including patient-derived xenografts, to accelerate the drug screening process and drive clinical translation of personalized medicines.
- Further studies might include quantification of antigen presentation by bioprinted tumor cells, T cell infiltration into the tumors and cytokine expression by T cells.
- Additionally, the multiwell bioprinting format on the BIO X could be used to scale up support for high-throughput screening of biological agents (such as immune checkpoint inhibitors) and engineered T cells (CAR-T).

References

1. Budhu, S., Loike, J. D., Pandolfi, A. CD8+ T cell concentration determines their efficiency in killing cognate antigen-expressing syngeneic mammalian cells in vitro and in mouse tissues. *Journal of Experimental Medicine*. 2010; 207(1): 223–235. [DOI: 10.1084/jem.20091279](https://doi.org/10.1084/jem.20091279).
2. Golstein, P. and Griffiths, G. M. An early history of T cell-mediated cytotoxicity. *Nature Reviews Immunology*. 2018; 18(8): 527–535. [DOI: 10.1038/s41577-018-0009-3](https://doi.org/10.1038/s41577-018-0009-3).
3. Jenkins, R. W., Aref, A. R., Lizotte, P. H., et al. Ex vivo profiling of PD-1 blockade using organotypic tumor spheroids. *Cancer Discovery*. 2018; 8(2): 196–215. [DOI: 10.1158/2159-8290.CD-17-0833](https://doi.org/10.1158/2159-8290.CD-17-0833).
4. Nath, S., Christian, L., Tan, S. Y., et al. Dynein separately partners with NDE1 and dynactin to orchestrate T cell focused secretion. *Journal of Immunology*. 2016; 197(6): 2090–2101. [DOI: 10.4049/jimmunol.1600180](https://doi.org/10.4049/jimmunol.1600180).
5. Sharon, E., Streicher, H., Goncalves, P., and Chen, H. X. Immune checkpoint inhibitors in clinical trials. *Chinese Journal of Cancer*. 2014; 33(9): 434–444. [DOI: 10.5732/cjc.014.10122](https://doi.org/10.5732/cjc.014.10122).
6. Steff, A.-M., Fortin, M., Arguin, C., and Hugo, P. Detection of a decrease in green fluorescent protein fluorescence for the monitoring of cell death: An assay amenable to high-throughput screening technologies. *Cytometry*. 2001; 45(4): 237–243. [DOI: 10.1002/1097-0320\(20011201\)45:4<237::AID-CYTO10024>3.0.CO;2-J](https://doi.org/10.1002/1097-0320(20011201)45:4<237::AID-CYTO10024>3.0.CO;2-J).
7. Strebel, A., Harr, T., Bachmann, F., et al. Green fluorescent protein as a novel tool to measure apoptosis and necrosis. *Cytometry*. 2001; 43(2): 126–133. [DOI: 10.1002/1097-0320\(20010201\)43:2<126::AID-CYTO1027>3.0.CO;2-J](https://doi.org/10.1002/1097-0320(20010201)43:2<126::AID-CYTO1027>3.0.CO;2-J).
8. Topalian, S., Taube, J., Anders, R. et al. Mechanism-driven biomarkers to guide immune checkpoint blockade in cancer therapy. *Nature Reviews Cancer*. 2016; 16(5): 275–287. [DOI: 10.1038/nrc.2016.36](https://doi.org/10.1038/nrc.2016.36).

Contact Us

US phone:
(+1) 833-235-5465

European phone:
+46 31-128 700

Email:
sales@cellink.com

Website:
www.cellink.com



© 2020 CELLINK AB. All rights reserved. Duplication and/or reproduction of all or any portion of this document without the express written consent of CELLINK is strictly forbidden. Nothing contained herein shall constitute any warranty, express or implied, as to the performance of any products described herein. Any and all warranties applicable to any products are set forth in the applicable terms and conditions of sale accompanying the purchase of such product. CELLINK provides no warranty and hereby disclaims any and all warranties as to the use of any third-party products or protocols described herein. The use of products described herein is subject to certain restrictions as set forth in the applicable terms and conditions of sale accompanying the purchase of such product. CELLINK may refer to the products or services offered by other companies by their brand name or company name solely for clarity and does not claim any rights to those third-party marks or names. CELLINK products may be covered by one or more patents. The use of products described herein is subject to CELLINK's terms and conditions of sale and such other terms that have been agreed to in writing between CELLINK and user. All products and services described herein are intended FOR RESEARCH USE ONLY and NOT FOR USE IN DIAGNOSTIC PROCEDURES.

The use of CELLINK products in practicing the methods set forth herein has not been validated by CELLINK, and such nonvalidated use is NOT COVERED BY CELLINK'S STANDARD WARRANTY, AND CELLINK HEREBY DISCLAIMS ANY AND ALL WARRANTIES FOR SUCH USE. Nothing in this document should be construed as altering, waiving or amending in any manner CELLINK's terms and conditions of sale for the instruments, consumables or software mentioned, including without limitation such terms and conditions relating to certain use restrictions, limited license, warranty and limitation of liability, and nothing in this document shall be deemed to be Documentation, as that term is set forth in such terms and conditions of sale. Nothing in this document shall be construed as any representation by CELLINK that it currently or will at any time in the future offer or in any way support any application set forth herein.